Calculation of the transonic flow in a plane channel using a low Reynolds $k-\varepsilon$ turbulence model

L. Davidson
CERFACS
42, Av. Gustave Coriolis
31057 Toulouse
FRANCE
Report TR/RF/90/26, 1990

Introduction

The transonic flow in a two-dimensional plane channel is predicted. Two different turbulence models are used: the low Reynolds turbulence model by Chien [2], and the algebraic model by Baldwin and Lomax [1]. The predictions are compared with experiments by Delery [4], [6].

The work presented in this report has been carried out in the context of the EUROVAL project (validation of CFD codes) which is part of BRITE/EURAM.

Equations

The mean flow equations that are solved are the continuity equation, the momentum equations and the energy equation. The continuity equation can be written as:

$$\frac{\partial \rho}{\partial t} + \frac{\partial}{\partial x_j}(\rho U_j) = 0$$

The momentum equations and the equation for the total energy have the form:

$$\frac{\partial \rho U_i}{\partial t} + \frac{\partial}{\partial x_j}(\rho U_i U_j) = -\frac{\partial p}{\partial x_i} + \frac{\partial \tau_{ij}}{\partial x_j}$$

$$\frac{\partial \rho e_o}{\partial t} + \frac{\partial}{\partial x_i}[\rho U_i (e_o + p)] = \frac{\partial}{\partial x_i}(\tau_{ij} U_j + \frac{\mu_{eff}}{\sigma_e}\frac{\partial T}{\partial x_i})$$

where the stress tensor is written as:

$$\tau_{ij} = \mu(\frac{\partial U_i}{\partial x_j} + \frac{\partial U_j}{\partial x_i} - \frac{2}{3}\delta_{ij}\frac{\partial U_k}{\partial x_k}) - \rho\overline{u_i u_j}$$

The pressure is obtained from the gas law.

The Code

The code that has been used has the following characteristics [8], [5]

i) explicit, cell-centered finite volume, central differencing, local time stepping;

ii) fourth stage Runge-Kutta scheme for the mean-flow equations;

iii) the k and ε equations are solved using a semi-implicit solver [3] (hybrid central/upwind scheme, ADI);

iv) forth-order numerical non-homogenous dissipation term in all mean flow equations [9] (no shock capturing second order term).

Turbulence Models

Two turbulence models are used: the standard Baldwin-Lomax model [1] (including the intermittency function) and the low Reynolds $k-\varepsilon$ turbulence model by Chien [2]. The $k-\varepsilon$ model has the following form:

$$\frac{\partial}{\partial x_j}(\rho U_j k) = \frac{\partial}{\partial x_j}(\mu + \frac{\mu_t}{\sigma_k})\frac{\partial k}{\partial x_j} + P_k - \rho\varepsilon - 2\mu\frac{k}{y^2}$$

$$\frac{\partial}{\partial x_j}(\rho U_j \varepsilon) = \frac{\partial}{\partial x_j}(\mu + \frac{\mu_t}{\sigma_\varepsilon})\frac{\partial \varepsilon}{\partial x_j} + \frac{\varepsilon}{k}(c_{1\varepsilon}P_k - c_{2\varepsilon}f_2\rho\varepsilon) - 2\mu\frac{\varepsilon}{y^2}exp(-0.5y^+)$$

where

$$P_k = \frac{\partial U_i}{\partial x_j}[\mu_t(\frac{\partial U_i}{\partial x_j} + \frac{\partial U_j}{\partial x_i} - \frac{2}{3}\delta_{ij}\frac{\partial U_m}{\partial x_m}) - \frac{2}{3}\delta_{ij}\rho k]$$

The turbulent viscosity is calculated as

$$\mu_t = \frac{c_\mu f_\mu \rho k^2}{\varepsilon}$$

which gives the Reynolds stress tensor

$$\rho\overline{u_i u_j} = -\mu_t(\frac{\partial U_i}{\partial x_j} + \frac{\partial U_j}{\partial x_i} - \frac{2}{3}\delta_{ij}\frac{\partial U_m}{\partial x_m}) + \frac{2}{3}\delta_{ij}\rho k$$

Standard values on the constants have been used: $c_\mu = 0.09$, $c_1 = 1.35$, $c_2 = 1.8$.

Mesh

A mesh with 121 lines in the x-direction (from $x/L = -0.35$ to $x/L = 2$; L denotes the length of the bump), and 81 in the (normal) y-direction. In the x-direction constant spacing, $\delta x/L = 0.023$, is used for $-0.35 \leq x/L \leq 0.6$; for $0.6 \leq x/L \leq 0.7$, $0.9 \leq x/L \leq 1.0$ δx is divided by two, and for $0.7 \leq x/L \leq 0.9$ δx is divided by four. In the y-direction δy is increased by a factor 1.1 when y increases. This gives a y-value of $y/L = 6.1 \cdot 10^{-6}$ for the first grid node, and y^+ which vairies between 0.1 and 1.3. The maximum δy close to the centerline is $y/L = 0.023$

Boundary Conditions

Inlet

Total temperature and total pressure are prescribed. V is set to zero and the density is extrapolated from inside. The U-velocity and the total energy are set as:

$$U = \sqrt{2RT_o[1 - (\frac{\rho}{\rho_o})^{\gamma-1}]\frac{\gamma}{\gamma-1}}$$

$$e_o = \frac{RT_o}{\gamma-1}(\frac{\rho}{\rho_o})^{\gamma-1}\frac{U^2}{2}$$

The turbulent kinetic energy and its dissipation are set using the mixing length

$$\ell = min\{\kappa y(1 - exp(y^+/26), 0.09H/2\}$$

(H denotes the height of the channel) and a turbulent velocity scale

$$\mathcal{U} = \ell\frac{\partial U}{\partial y}$$

so that

$$k = \mathcal{U}^2$$

and

$$\varepsilon = c_\mu^{3/4}\frac{\mathcal{U}^2}{\ell}$$

Outlet

At the outlet the Riemann invariants are used which are based on the theory of characteristics for the locally one-dimensional problem. The four Riemann invariants are:

$$
\begin{aligned}
R_1 &= \mathbf{U} \cdot \mathbf{n} - \frac{2}{\gamma - 1} c \\
R_2 &= \mathbf{U} \cdot \mathbf{n} + \frac{2}{\gamma - 1} c \\
R_3 &= ln(\frac{p}{\rho^\gamma}) \\
R_4 &= n_y U - n_x V
\end{aligned}
$$

where $\mathbf{n}$ and c denote normal vector and speed of sound, respectively. The normal gradients of the Riemann invariants are set to zero, i.e.

$$
\frac{\partial R_m}{\partial x} = 0
$$

R_1 is taken from outside and R_2, R_3 and R_4 from inside. R_3 gives the density since the pressure $\frac{p}{p_o} = 0.654$ is given (this modified outlet pressure was chosen in the EUROVAL project). R_4 gives that the tangential velocity , i.e. $\frac{\partial V}{\partial x} = 0$. Finally, knowing the speed of sound both inside and outside, R_2 gives the U-velocity.

Wall

At the wall ρU, ρV, k, and ε are set to zero. Furthermore the normal gradients of pressure and temperature are set to zero.

Convergence Data

10 000 iterations were used for both turbulence models. The residuals R are defined as the sum of the absolute right-hand-side (the left-hand-side contains only the time derivative) of the equations summed for all cells. This is scaled with the total inflow amount S [$(\dot{m})_{in}$ for continuity equation, $(\dot{m}U)_{in}$ for momentum equations, and $(\dot{m}e_o)_{in}$ for total energy]. The residuals can be written

$$
R_q = \frac{1}{S} \sum_{ij} \mid R.H.S. \mid
$$

where R_q denotes the residual for variable q [$q = \rho, \rho U, ..$].

$k - \varepsilon$ Model

The residuals were, after 10 000 iteration, $2.5 \cdot 10^{-4}$, $8.0 \cdot 10^{-4}$, $4.2 \cdot 10^{-5}$, for the continuity, momentum, and energy equation respectively. The CPU time on a FX/80 Alliant was 4.2 hours.

Baldwin-Lomax Model

The residuals were, after 10 000 iteration, $3.7 \cdot 10^{-4}$, $1.2 \cdot 10^{-3}$, $1.2 \cdot 10^{-4}$, for the continuity, momentum, and energy equation respectively. The CPU time on a FX/80 Alliant was 3.3 hours.

Problems

In the beginning the explicit Runge-Kutta solver was used for the k and ε equations. Serious convergence problems were, however, encountered, and no stable solution was obtained. To remedy this problem the k and ε equations are solved semi-implicitly in the same way as in codes using SIMPLE-methods [7]; the main characteristics are hybrid central/upwind differencing, and Three-Diagonal-Matrix-Algorithm for solving the resulting linear equations in both coordinate directions. The $k-\varepsilon$ turbulence model is now very stable and does not cause any convergence problems.

Initially the inlet was placed at $x = 0$, i.e. at the beginning of the bump. This resulted in negative U-velocities in the corner near the inlet and the wall. In order to avoid this the inlet was placed at $x/L = -0.35$.

Results

In Fig.1 the configuration together with the grid is presented.

The pressure distributions are shown in Fig.2, and it can be seen that for the chosen exit pressure the location of the shock is better predicted with the $k-\varepsilon$ model than with the Baldwin-Lomax model.

The predicted center-line Mach number obtained with the $k-\varepsilon$ model is compared with the experimental values in Fig.3, which further confirms the correct position of the shock. It can be seen that near the shock some under-shoots and over-shoots appear. This is because no second order shock capturing term is used. This is further illustrated in Fig.4 where the calculated wall pressure and the center-line pressure are compared with the experimental wall-pressure. At the center-line where the viscos effects are small (laminar viscosity), the natural viscosity does not manage to damp the pressure occilations. In Fig.5 the pressure at $y/L = 6.4 \cdot 10^{-4}$ (grid line J=20), $y/L = 4.9 \cdot 10^{-4}$ (J=40), and $y/L = 0.034$ (J=60) are plotted, and it can be seen that no over-shoots or under-shoots appears, which indicates that the "natural" (i.e the turbulent) viscosity is, in the boundary layer, sufficient to damp any occilations in the pressure near the shock.

The shock is slightly deflected as the wall is approached as can be seen in Fig.6, and at the shock there is a strong production of turbulent kinetic energy (see Fig.7).

The predicted displacement thicknesses are compared with the experimental

one in Fig. 8. The displacement thickness is defined as:

$$\delta_1 = \int_0^\infty (1 - \frac{\rho}{\rho_\infty}\frac{u}{u_\infty})dy$$

The predictions with the $k-\varepsilon$ model are in closer agreement with experiments than those obtained with the Baldwin-Lomax model. The discrepancy between the predicted and experimental values is, ahead of the shock, large for both models. These discrepancies are due to the strong variations of the density where the "free-stream" values ρ_∞, for a given x, is smaller than the density in the boundary layer due to the small deflection of the shock near the wall (see Fig. 6), which even gives negativ δ_1-values.

The velocity profiles are presented in Fig.9. At the first station, well ahead of the shock, the agreement is good for both models. At $x/L = 0.775$, which is still ahead of the shock, the boundary is approaching the shock and its thickness is growing (Fig. 9b). Figs. 9c-e shows how the velocity profiles changes when the flow is entering the shock. The two "bumps" in the velocity profiles in Figs. 9c,d show at which y coordinate, for the given x/L, the sligtly inclined shock (cf. Fig.6) is located: these "bumps" are due to the strong variations in density ($\partial\rho/\partial x$ is very large) at the shock (the code solves for ρU and U is obtained by dividing by ρ). In Fig.9e the flow near the wall ($y/L \leq 0.06$) has passed through the shock whereas further away from the wall the flow is entering the shock (cf. Fig.6). At $x/L = 0.8$ the profile predicted with the Baldwin-Lomax model is still ahead of the shock, and at $x/L = 0.825$ the flow predicted with the Baldwin-Lomax model is just about to enter the shock , and the flow predicted with the $k-\varepsilon$ model has passed through the shock. In Fig.9g the velocity profiles predicted with the two models are, again, very similar. It can be seen, however, that the predicted velocities are smaller than the experimental ones. This is because the predicted pressure level is to high (see Fig.2) which gives to high values on the density, which, due to mass conservation, gives to small a velocity. This was confirmed in calculations carried out prescribing the experimental outlet pressure $\frac{p}{p_o} = 0.64$, where the calculated velocities at the outlet agrees well with the experimental ones.

In Fig.10 the turbulent kinetic energy profiles are shown. At the first station the calculated profile agrees well with experiments. As the shock is approached both calculated and experimental values increase. The production of turbulent kinetic energy is, however, stronger in the experiments than in the calculations. Furthermore, the maxima of the profiles are located further away from the wall in the experiments that in the calculations. Far downstream the bump the predicted values are still smaller than the experimental ones. It may be noted that the predicted profile far downstream exhibits the, for fully developed boundary layer flow, characteristic peak close to the wall.

Conclusions

A low Reynolds number $k-\varepsilon$ model and a Baldwin-Lomax turbulence model have been used to calculate the transonic flow in a plane channel. For the predictions with the $k-\varepsilon$ model the following conclusions can be drawn:

- for the chosen outlet pressure the location of the shock is predicted according to experiments
- the predicted displacement thickness and the velocity profiles are well in agreement with the experiments
- in, and after, the chock region the turbulent kinetic energy is higher in the experiments than in the predictions
- in the absence of a second-order shock capturing term occilations appear in the pressure in the shock region near the center-line where the viscos effects are small; in the boundary layer, however, it is shown that the total viscosity (turbulent plus laminar) is sufficient to damp these pressure occilations

The predicted location of the shock with the Baldwin-Lomax model is too late compared with experiments. It should be remembered that the outlet pressure used in this work has been modified and is thus not the same as in the experiments. This modified outlet pressure was chosen in the EUROVAL project based on calculations carried out with $k-\varepsilon$ models; if the experimental outlet pressure were used the location of the shock would be predicted too late also with the $k-\varepsilon$ model. But, evidently, the exit pressure has to be modified (i.e. increased) more for the Baldwin-Lomax model than for the $k-\varepsilon$ model. It can thus be concluded that the Baldwin-Lomax does not give as good results as does the $k-\varepsilon$ model.

References

[1] **B. BALDWIN and H. LOMAX** *Thin-Layer Approximation and Algebraic Model for Separated Turbulent Flows*, AIAA Paper No 78-257, January 1978.

[2] **K.Y. CHIEN**, *Predictions of Channel and Boundary Layer Flows with a Low-Reynolds-Number Turbulence Model*, AIAA Journal, **20**, 33-38, 1982.

[3] **L. DAVIDSON**, *Implementation of a Semi-Implicit $k-\varepsilon$ Turbulence Model in a Explicit Runge-Kutta Navier-Stokes Code*, Rept. TR/RF/90/25, CERFACS, 1990.

[4] **J. DÉLERY**, *Experimental Investigation of Turbulence Properties in Transonic Shoch/Boundary Layer Interactions*, AIAA J., **21**, 180-185, 1983.

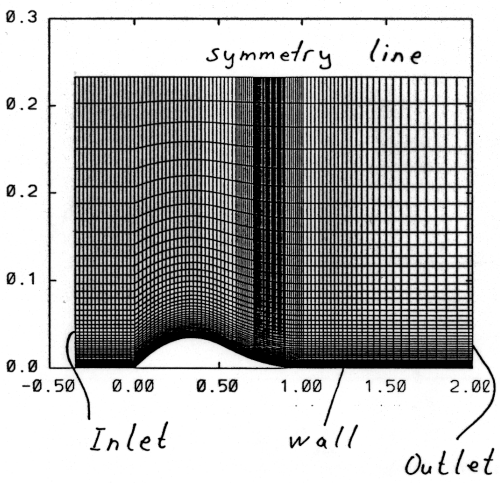

Figure 1: *Configuration with grid. Note that different scales are used in x and y-directions.*

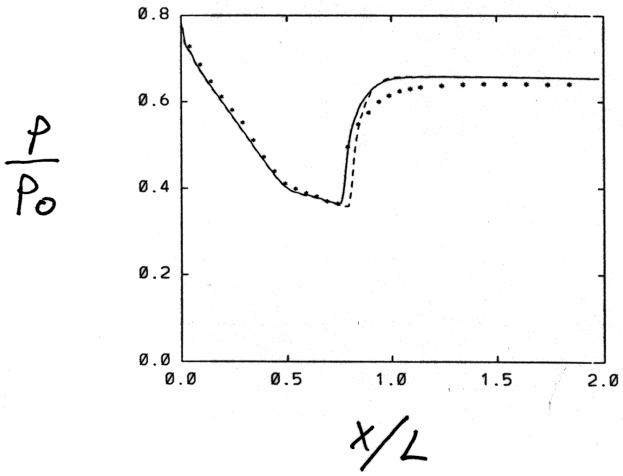

Figure 2: *Wall pressure. Solid line: $k-\varepsilon$; dashed line: Baldwin-Lomax; markers: experiments.*

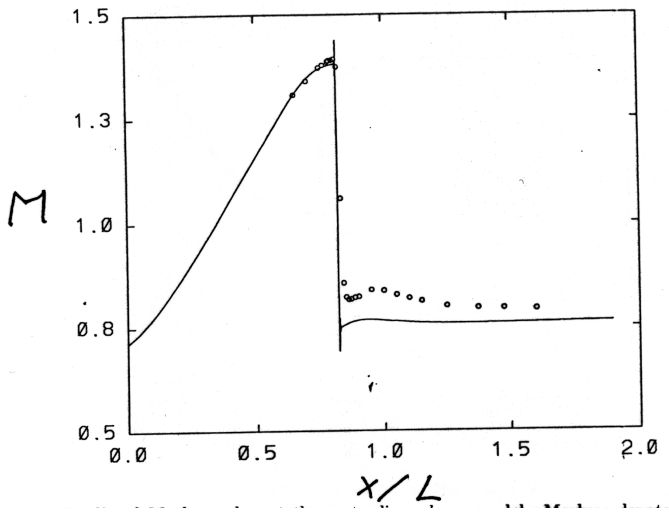

Figure 3: *Predicted Mach number at the center-line. $k-\varepsilon$ model. Markers denote experimental Mach number.*

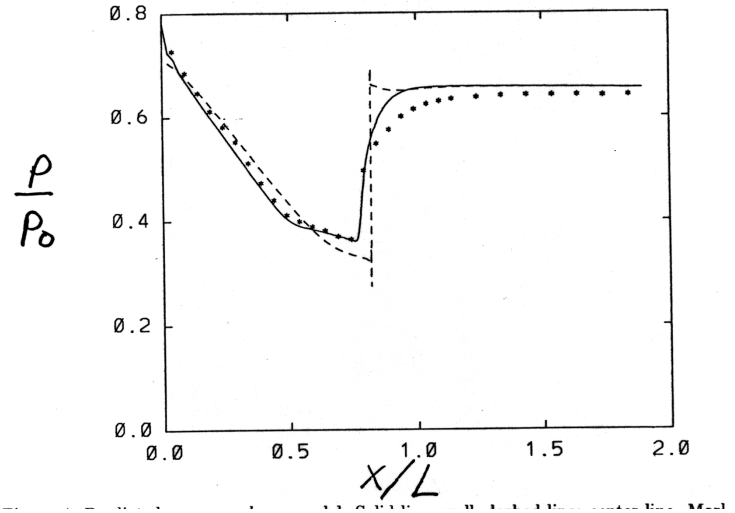

Figure 4: *Predicted pressure. $k-\varepsilon$ model. Solid line: wall; dashed line: center-line. Markers denote experimental wall pressure.*

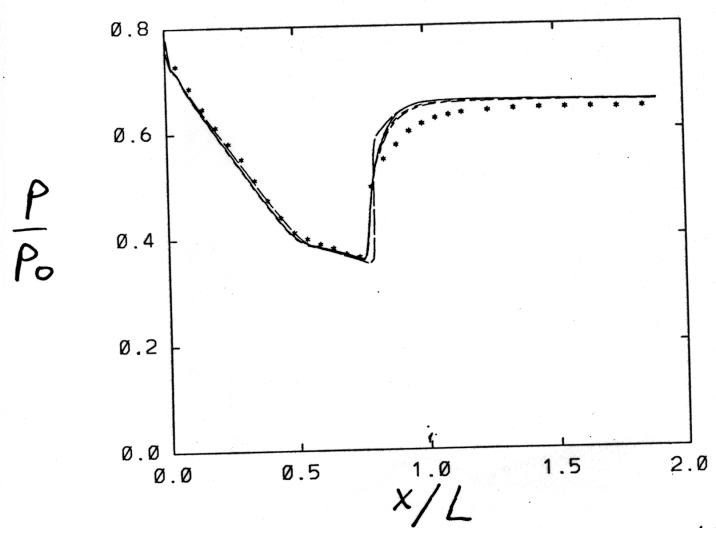

Figure 5: *Predicted pressure, with the* $k-\varepsilon$ *model, at the wall,* $y/L = 6.4 \cdot 10^{-4}$ *(grid line J=20),* $y/L = 4.9 \cdot 10^{-4}$ *(J=40), and* $y/L = 0.034$ *(J=60). Markers denote experimental wall pressure.*

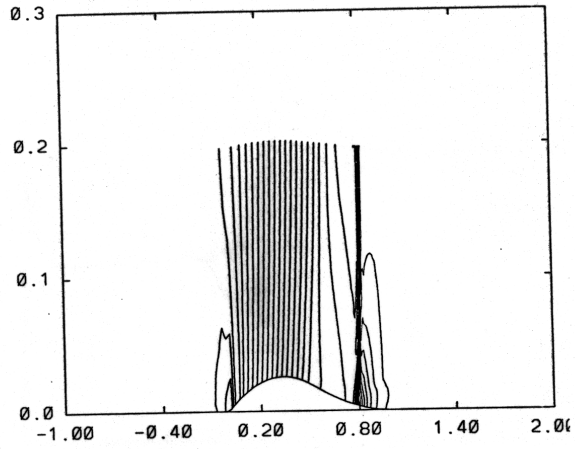

Figure 6: *Iso-contours of pressure.* $k-\varepsilon$ *model. Note that different scales are used in* x *and* y*-directions.*

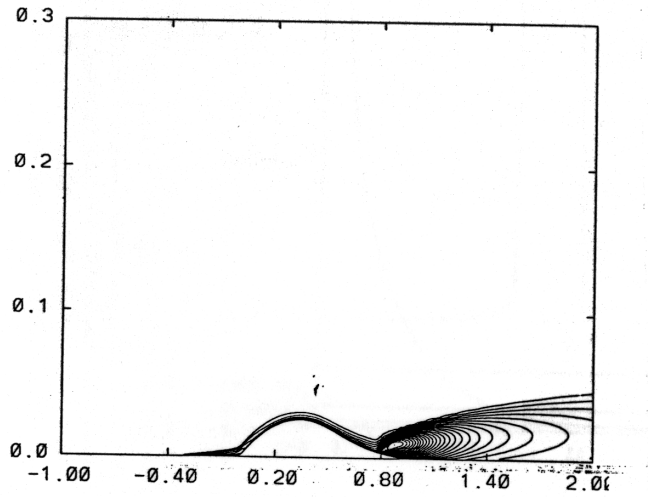

Figure 7: *Iso-contours of turbulent kinetic energy. Note that different scales are used in x and y-directions.*

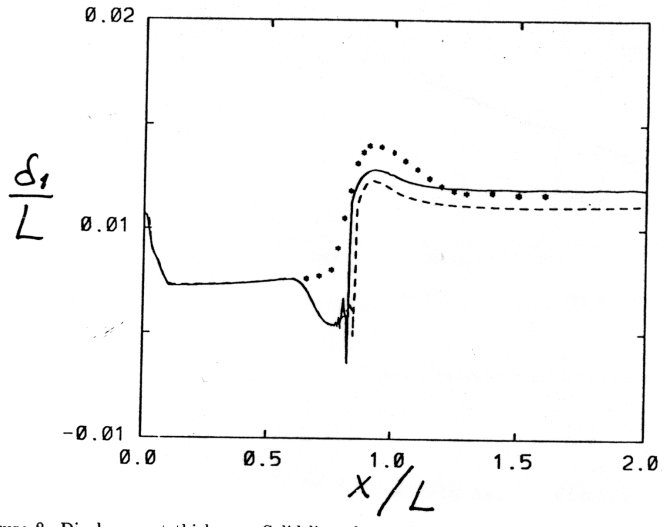

Figure 8: *Displacement thickness. Solid line: $k-\varepsilon$; dashed line: Baldwin-Lomax; markers: experiments.*

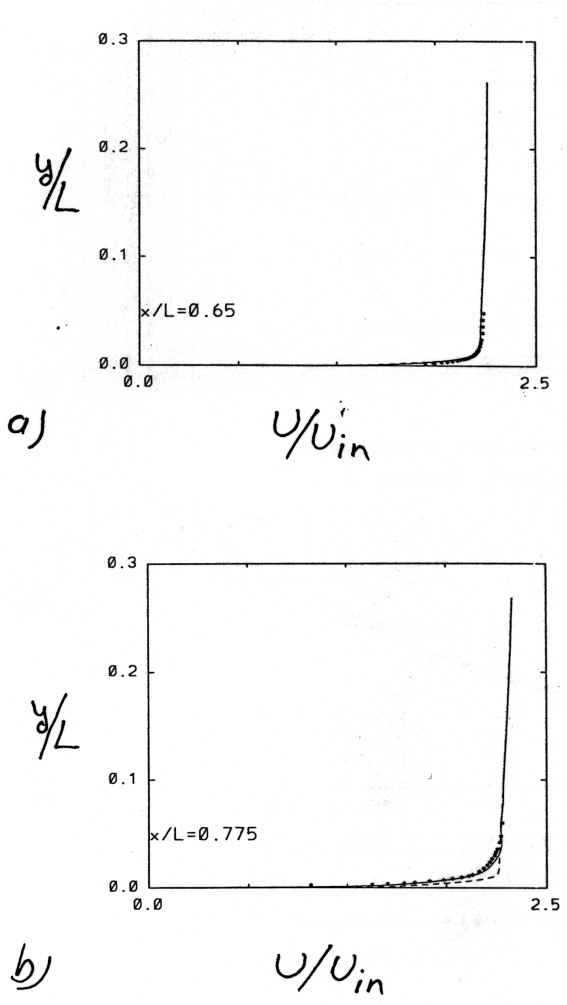

Figure 9: *U velocity profiles. Solid line:* $k-\varepsilon$*; dashed line: Baldwin-Lomax; markers: experiments. a)* $x/L = 0.65$*, b)* $x/L = 0.775$.

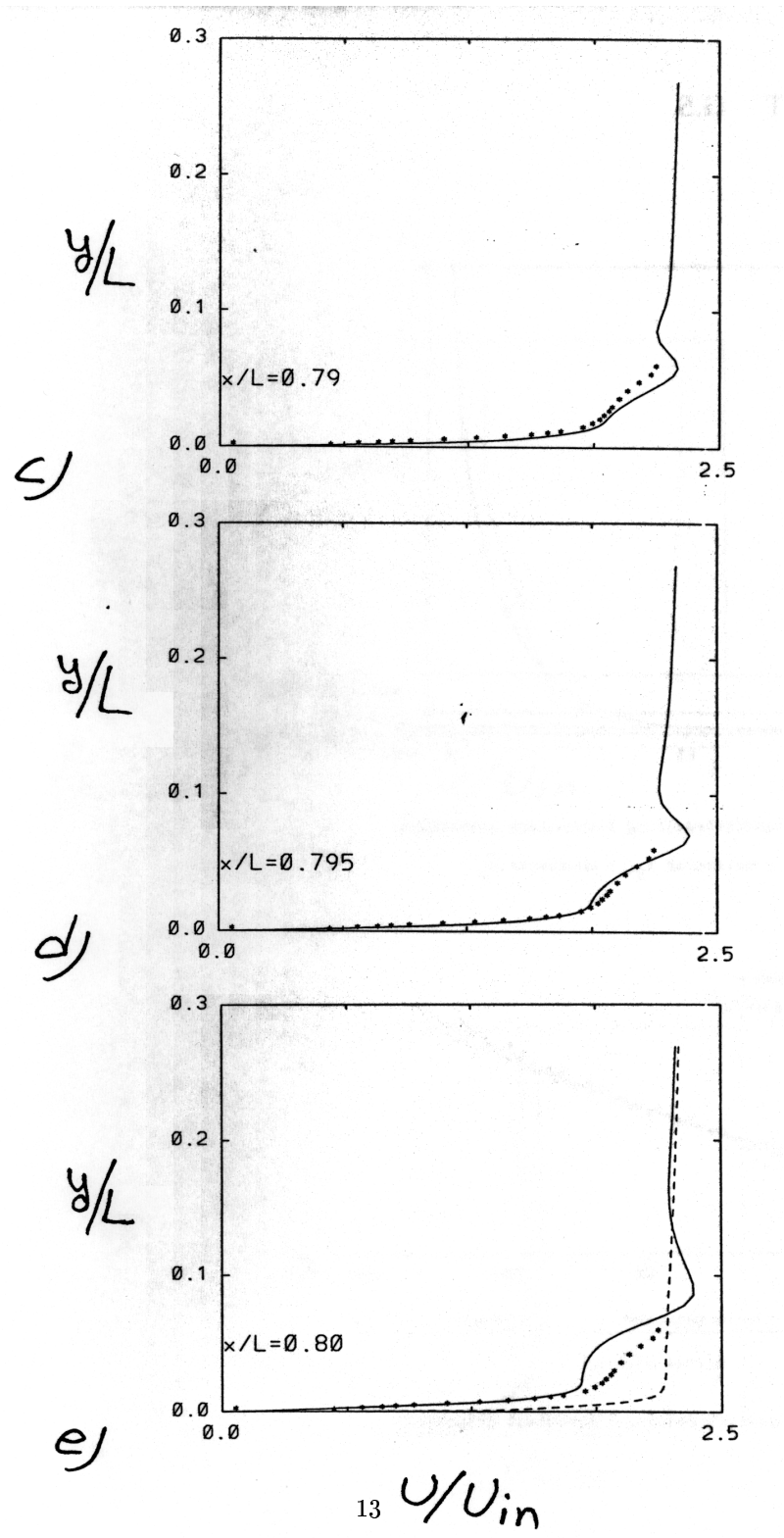

Figure 9: *(cont'd). U velocity profiles. Solid line:* $k-\varepsilon$*; dashed line: Baldwin-Lomax; markers: experiments. (note that the experimental values in Fig. 5c-d are all taken at* $x/L = 0.8$*) c)* $x/L = 0.79$ *(only* $k-\varepsilon$ *model), d)* $x/L = 0.795$ *(only* $k-\varepsilon$ *model), e)* $x/L = 0.80$*.*

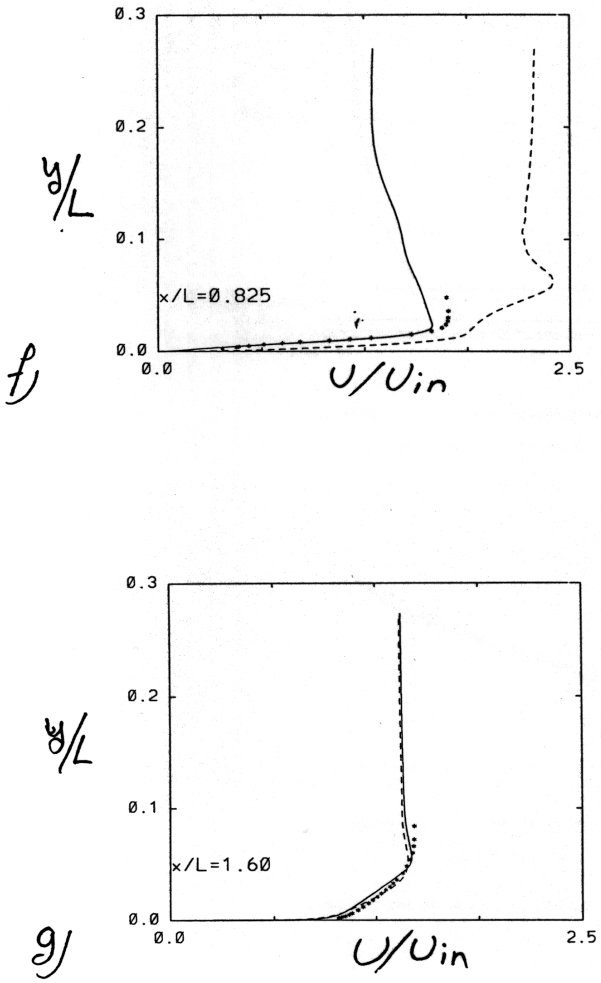

Figure 9: *(cont'd). U velocity profiles. Solid line:* $k-\varepsilon$*; dashed line: Baldwin-Lomax; markers: experiments. f)* $x/L = 0.825$*, g)* $x/L = 1.60$.

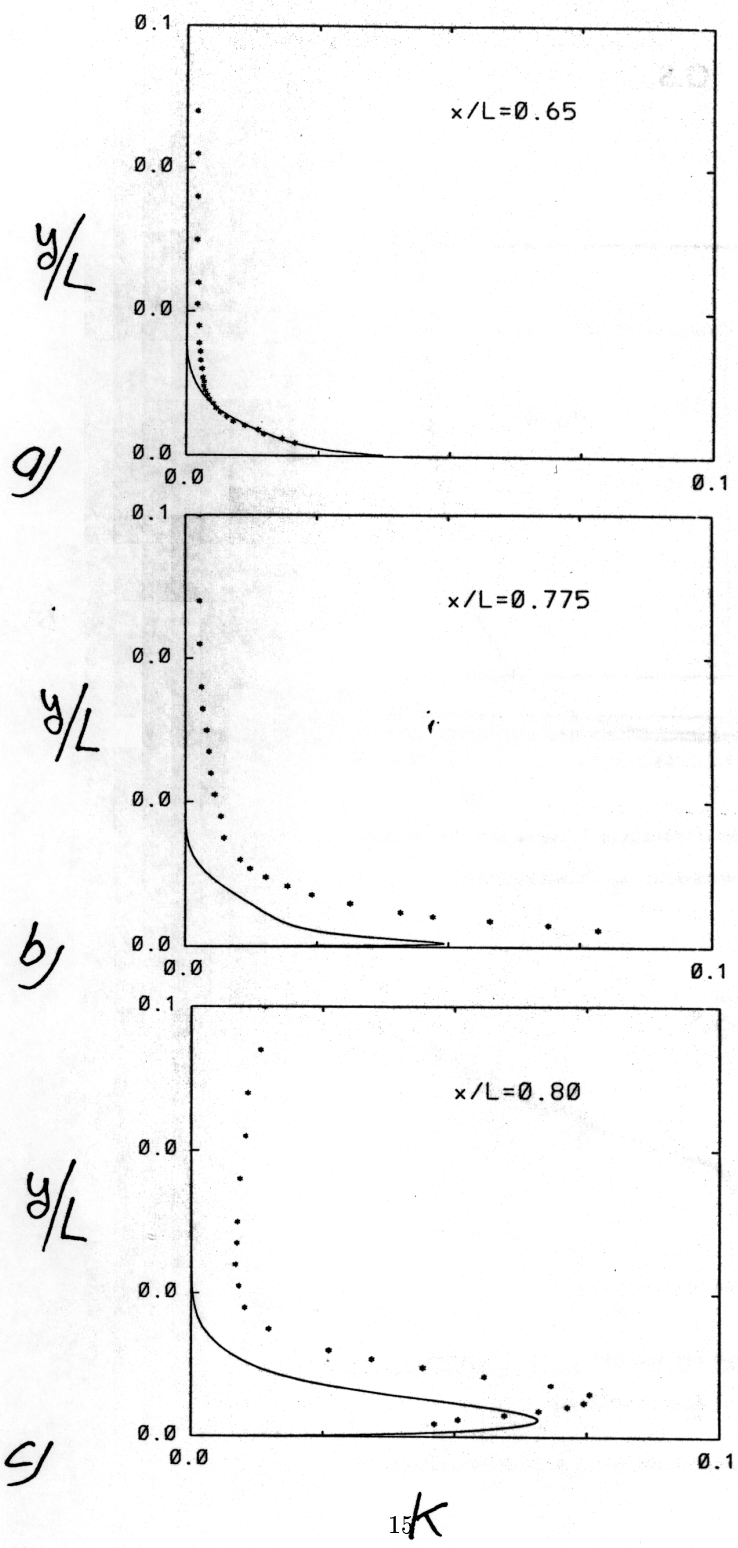

Figure 10: *Profiles of turbulent kinetic energy. Solid line:* $k-\varepsilon$*; markers: experiments. a)* $x/L = 0.65$*, b)* $x/L = 0.775$*, c)* $x/L = 0.80$.

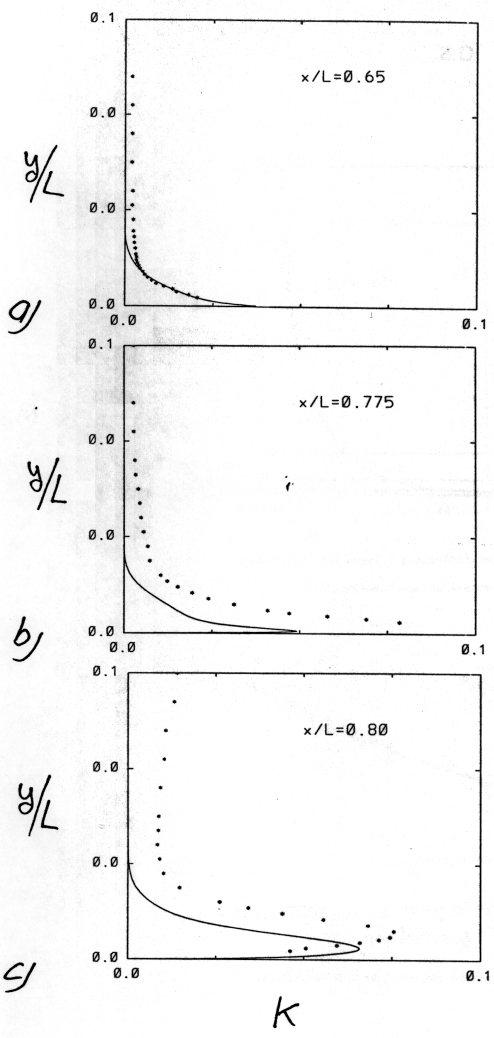

Figure 10: *(cont'd). Profiles of turbulent kinetic energy. Solid line:* $k-\varepsilon$*; markers: experiments. d)* $x/L = 0.85$*, e)* $x/L = 1.6$.

[5] **B. MÜLLER and A. RIZZI**, *Runge-Kutta Finite Volume Simulation of Transonic Flow Over a NACA0012 Airfoil using the Navier-Stokes Equations*, FFA TN 1986-60, 1986

[6] ONERA Rapport Technique No. 42/7078 AY 014, December 1980.

[7] **S.V. PATANKAR** *Numerical Heat Transfer and Fluid Flow*, McGraw-Hill, New York, 1980.

[8] **A. RIZZI and B. MÜLLER** *Large-Scale Viscous Simulation of Laminar Vortex Flow Over a Delta Wing*, AIAA Journal, **27**, 833-840, 1989.

[9] **R.C. SWANSON and E. TURKEL** *Artificial Dissipation and Central Difference Schemes for the EULER and NAVIER-STOKES Equations*, AIAA Paper No 87-1107, 1987.